Improved performance of perovskite solar cells through using $(FA)_x(MA)_{1-x}PbI_3$ optical absorber layer*

SUI Mei-rong (隋美蓉)[1]**, **LI Sheng-ping** (李省平)[2], **and GU Xiu-quan** (顾修全)[2]
1.School of Medical Imaging, Xuzhou Medical University, Xuzhou 221004, China
2.School of Materials Science and Engineering, China University of Mining and Technology, Xuzhou 221116, China

(Received 23 July 2018; Revised 13 August 2018)

In this work, the perovskite solar cells (PSCs) were fabricated with the bandgap-tunable $(FA)_x(MA)_{1-x}PbI_3$ absorber layers through a facile two-stage deposition route. The doping was realized by adding the formamidinium iodide (FAI) into a precursor MAI solution. Both the surface morphology and electrochemical impedance spectra (EIS) were conducted to evaluate the absorber layers or solar cells. After the optimization, the best PSC performance of 14.73% was achieved at a nominal FAI content of 12.5 at.%. The performance enhancement was attributed to both the enhancement of visible light harvesting and carrier transport capability. Besides, the stability of a PSC device based on the single $MAPbI_3$ absorber layer was also investigated, and a power conversion efficiency (*PCE*) of 11.27 % remained even after laying in vacuum for 10 days.

Document code: A **Article ID:** 1673-1905(2019)02-0117-5
DOI https://doi.org/10.1007/s11801-019-8118-1

Recently, perovskite solar cells (PSCs) have received worldwide attention since 2012[1-3]. The power conversion efficiency (*PCE*) of the PSCs has soared from 3.8% to 21.6% in the laboratory level (with a small active area of 0.1 cm^2)[4, 5], which is very close to the level of traditional Si based solar cells. Overall, several problems must be solved before the actual application of the PSCs, e.g., the removal of harmful elements (Pb), the suppression of a *J-V* hysteresis, the improvement of long-term stability, the increase of single device size, and so on. In a latest reference, a research group reported the fabrication of a large-area, mesoporous TiO_2-based perovskite solar module (~36.1 cm^2) through a solvent- and vacuum-free route, and achieved a certified *PCE* of 12.1%[6]. Besides, Bush and his coworkers demonstrated a recorded *PCE* of 23.6% from the monolithic, two-terminal, 1 cm^2 perovskite/silicon tandems recently, as well as the improved thermal and environmental stability through undergoing a 1 000 h damp heat test at 85 °C and 85% relative humidity[7]. And also in a few latest reports, the PSCs have been used for constructing an integrated solar water splitting tandem device with the earth-abundant electrocatalysts, or photoelectrodes (e.g., α-Fe_2O_3, $BiVO_4$, etc.)[8-10].

In fact, the PSC is a pn heterojunction device, which is usually made up of a fluorine-doped tin oxide (FTO) contact layer, a compact layer (CL), a mesoporous layer, a perovskite ($CH_3NH_3PbI_3$) absorber layer, a hole transporting material (HTM), and an Ag or Au counter electron layer. Under a solar illumination, the photoexcited carriers are separated by the built-in electric field formed at the semiconductor (e.g., TiO_2, SnO_2 or Al_2O_3)/perovskite interfaces, leading to a highly efficient conversion of solar to electric energy. And also, in a few studies, the mesoporous layer was absent in the device structure, and the resulting photovoltaic (PV) device was called as the planar PSCs[11,12]. For instance, Jung et al[11] reported the preparation of a solution-processed SnO_2 thin film for a hysteresis-free planar PSC, which displayed a *PCE* of 19.2%. The perovskite absorption layer is a crucial component in a PSC device, thus it is necessary to improve its crystalline quality for transporting the photo-generated carriers, or reduce its bandgap for more efficient visible light harvesting. It has been confirmed to be an efficient means to tune the bandgap of absorption layer by doping anions like Br^-, Cl^-, or the cations like a formamidinium ion (FA^+)[13-15]. However, there are still few reports on the cation doping of a $MAPbI_3$ absorption layer up to now.

In our previous studies, the main attention was focused on the optimization of TiO_2 CLs for enhancing the cell performance[16-18]. A high *PCE* of up to 15% has been demonstrated after an optimization of the preparation procedure. In this work, the composition of a perovskite ($MAPbI_3$) absorption layer is tuned continuously for enhancing the cell performance through a facile cation doping (with FA^+), leading to a 9.5% increase in the *PCE*.

CH_3NH_3I was synthesized by mixing and stirring

* This work has been supported by the Science and Technology Projects of Xuzhou City (No.KC14SM088), and the Natural Science Fund for Colleges and Universities in Jiangsu Province (No.15KJB430031).
** E-mail: smr2012@xzhmu.edu.cn

constantly 15 mL hydroiodic acid (HI, 57% in water, J&K) and 36 mL methylamine solution (CH_3NH_2, 33 wt% in ethanol, J&K) in a 250 mL round-bottomed flask at 0 °C for 3 h under N_2 atmosphere. The solvent was evaporated and the precipitate was washed with diethyl ether. Afterwards, the MAI powders were collected by drying the precipitate at 60 °C for 24 h in a vacuum oven. The PbI_2 (DMSO) solution was prepared exactly as described in Ref.[16], while the formamidinium iodide (CH_5N_2I, also said FAI) powders were purchased commercially from Sigma-Aldrich. The $(FA)_x(MA)_{1-x}I_3$ (also said FAMAI) precursor solution with a concentration of 14.8 mg/mL was prepared by dissolving the dry MAI and FAI powders into 2-propanol solvent at various MAI/FAI mass ratios. In details, the mass ratios of FAI to MAI/FAI were set as 0, 0.062 5, 0.125, 0.25, 0.50 and 1, respectively.

The FTO coated glass substrates (Pilkington, TEC 15) were partially etched with Zn powder and 2 mol/L HCl to form the electrode pattern. Then, the substrate was cleaned with deionized water, ethanol, isopropanol and absolute ethyl alcohol for 20 min in sequence. A 50-nm-thick TiO_2 CL was deposited on the F-doped SnO_2 glass (FTO, provided by Wuhan Jingge Ltd.) by spin-coating a TiO_2 precursor at 4 500 rpm for 30 s, which was followed by a heating process at 450 °C for 30 min in a muffle. Herein, the TiO_2 precursor was prepared by diluting titanium diisopropoxide bis(acetylacetonate) in 2-propanol solvent, leading to a 20 mmol/L dilute solution for spin-coating. Afterwards, a mesoporous TiO_2 layer was spun onto the CL by using a TiO_2 paste (Dyesol 18NRT, diluted in ethanol with a weight ratio of 1:5.5, J&K) at 5 000 rpm for 30 s, followed by a calcination treatment at 500 °C for 30 min.

Perovskite $FAMAPbI_3$ absorber layers were then deposited via a facile two-step drop-coating strategy (similar to a latest report from our group[17]), where FAMAI solution in 2-propanol (14.8 mg/mL) was used as the precursor instead of the commonly used MAI. In brief, a 1.25 mol/L PbI_2 (DMSO) solution was drop-coated onto the mesoporous TiO_2 layer at a speed of 3 200 rpm for 30 s. Then, the FAMAI solution was dropped onto the PbI_2 (DMSO) layer for 2 min, followed by a spinning process at 5 000 rpm for 30 s. Finally, the light black $TiO_2/MAPbI_3$ samples were heated on a hot plate at 145 °C for 18 min, which were then covered with an HTM layer by spinning HTM solution at a speed of 3 000 rpm for 30 s. Finally, a 70-nm-thick Ag layer was deposited as a counter electrode through a thermal evaporation under vacuum. A shadow mask was used for limiting the active area of device to a constant value of 0.1 cm^2.

The surface morphology and crystal structure of the $TiO_2/MAPbI_3$ layers were characterized by a field emission scanning electron microscope (FESEM, S-4800, Hitachi, Japan) and an X-ray diffractiometer (XRD, DX-2700B). The optical absorption spectra were characterized by a UV-Vis spectrophotometer (Varian Cary 300). The photocurrent density vs. voltage (*J-V*) plots of the obtained PSCs were recorded by a Keithley 2420 source meter under solar illumination (100 mW/cm^2, Oriel Sol 3A, Newport), which was calibrated by a standard silicon solar cell (Oriel Instrument), according to a latest report[19]. The incident-photon-to-current conversion efficiency (*IPCE*) was measured by using a power source (Newport 300 W Xe lamp, 66902) with a monochromator (Newport Cornerstone 260) and a power meter (Newport 2936-C). The electrochemical impedance spectra (EIS) of these PSCs were collected in dark at a voltage of 0.6 V by using a CHi-660 electrochemical workstation, and then the EIS data were analyzed by the Z-View software.

Fig.1 displays the macroscopical photographs of the obtained PSC devices in our lab. There are three devices on an FTO coated glass substrate for the *J-V* measurements, and a device located at the middle region is used for the performance evaluation. Besides, it is observed that the PSC device is semitransparent because the perovskite layer owns a limited thickness of ~500 nm and an optical bandgap of ~1.5 eV.

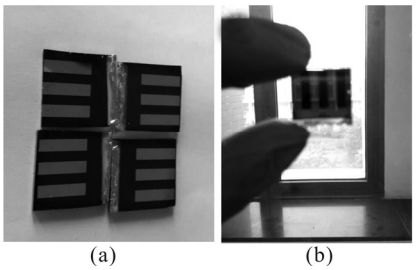

Fig.1 Typical digital photographs of the PSC devices fabricated in our lab

Fig.2 compares the top-view FESEM images of the perovskite absorber layers with various FA^+ doping contents. It is observed that the $MAPbI_3$ layer displays a polycrystalline morphology, although there are a few pinholes in the grain boundaries and a nonuniform distribution of the grain sizes. The doping of FAI into the precursor solution can suppress the pinholes efficiently, leading to an improvement of the film uniformity. Apparently, by a comparison, the sample with a 12.5% FAI content displays the highest quality, including the uniformity, smoothness and compactness. Nevertheless, when the FAI content exceeds 12.5%, a few small perovskite grains appear in the grain boundary regions, leading to both the deterioration of uniformity and compactness. When the FAI content reaches 100%, a lot of columns appear in the image, resulting in the poorest compactness of the $FAPbI_3$ absorber layers.

Fig.3 compares the XRD patterns of different perovskite absorbers. As could be seen, all the samples display the characteristic diffraction peaks of a perovskite $CH_3NH_3PbI_3$, while two dominant peaks (located at 14.2° and 28.47°) are identified as the (110) and (220) planes, respectively. The magnified XRD results in Fig.3(b) show that the (220) peak shifts towards the smaller angle side with increasing the FAI content in the perovskite, which is attributed to the lattice expansion caused by

an efficient FAI doping. When the FAI content reaches 100%, the (220) peak shifts towards 27.83°, corresponding to the lattice constant a=8.98 Å of single $FAPbI_3$. It is worth noting that the sample with an x value of 0.125 displays the highest intensity of (220) peak, suggesting the best crystalline quality of this sample.

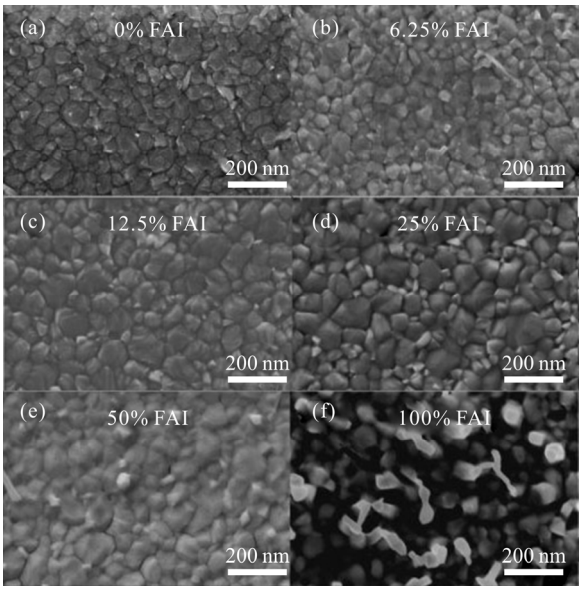

Fig.2 Typical FESEM images of $(FA)_x(MA)_{1-x}PbI_3$ (x=0—1) films: (a) x=0; (b) x=6.25%; (c) x=12.5%; (d) x=25%; (e) x=50%; (f) x=1

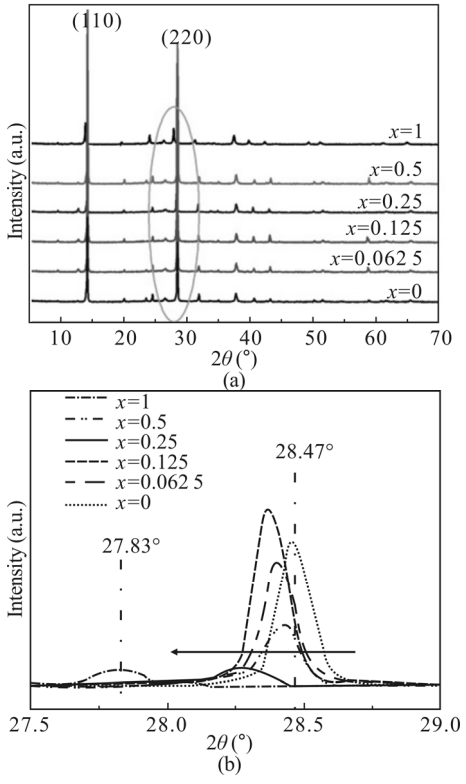

Fig.3 XRD patterns of perovskite $(MA)_{1-x}(FA)_xPbI_3$ (x=0—1) absorption layers in the ranges of (a) 5°—70° and (b) 27.5°—29.0°

Fig.4 compares the UV-Vis diffusion absorption spectra of various absorbers. Apparently, because $FAPbI_3$ displays a narrower bandgap (1.48 eV) than $MAPbI_3$ (1.57 eV), the FAI doping could enhance the visible-light absorption efficiently. As can be seen, not only the absorption edge is red shifted, but also the absorbance is enhanced significantly after the FAI doping.

Fig.5 displays the *J-V* plots of different PSC devices under solar irradiation, and the corresponding PV results (i.e., J_{SC}, V_{OC}, *FF* and *PCE*) are listed in Tab.1. The PSC devices fabricated with pure $MAPbI_3$ and $FAPbI_3$ absorber layers display poor *PCE* of 13.44% and 8.81%, respectively. With increasing the FA^+ content, the *PCE* is increased firstly and then decreased. The highest *PCE* is achieved at an FA^+ content of 12.5%. The performance enhancement results from both the improved J_{SC} and *FF* values, which might be associated with the broader absorption range and higher crystal quality of the absorber layers.

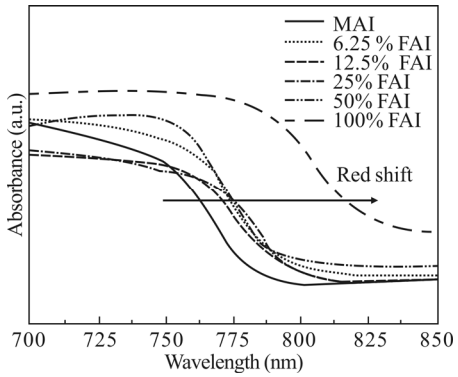

Fig.4 UV-Vis absorbance spectra of $(MA)_{1-x}(FA)_xPbI_3$ (x=0—1) perovskite absorber layers

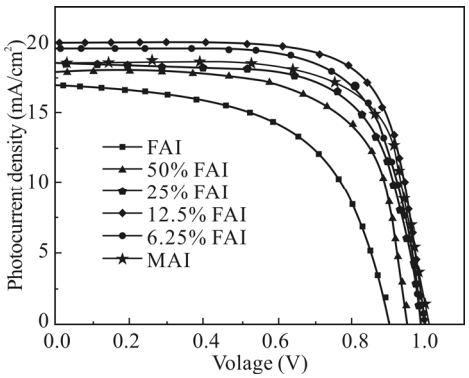

Fig.5 *J*−*V* plots of the devices based on perovskite $(FA)_x(MA)_{1-x}PbI_3$ (x=0—1) absorber layers (All the devices were measured under a solar irradiation intensity of 100 mW/cm^2 and an active area of 0.1 cm^2.)

Fig.6 compares the *IPCE* spectra of PSC devices fabricated using the pure and 12.5% FAI doped $MAPbI_3$ absorber layers. It is clear that the external quantum efficiency (*EQE*) values in 450—750 nm are enhanced significantly after the FAI doping, suggesting that the higher J_{SC} value is attributed to an enhancement of the visible-light absorption.

Tab.1 The electric parameters of TiO_2 PSCs with different FA doping contents under an AM 1.5 illumination (100 mW/cm^2)

Composition	J_{SC}/mA·cm^{-2}	V_{OC} / V	*FF* / %	*PCE*/%
MAI	18.6	1.0	71.8	13.4
6.25% FAI	19.6	0.99	70.3	13.7
12.5% FAI	20.0	0.99	74.0	14.7
25.0% FAI	18.6	0.98	69.2	12.6
50% FAI	17.9	0.95	68.0	11.6
100% FAI	17.0	0.90	57.4	8.8

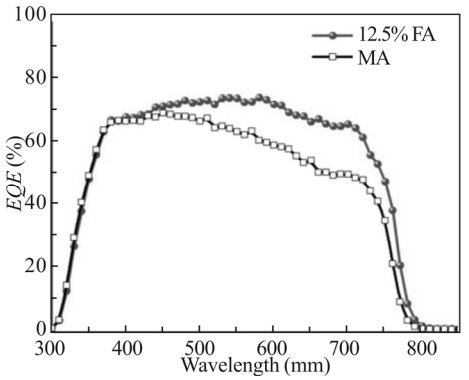

Fig.6 IPCE spectra of the devices based on perovskite $(FA)_x(MA)_{1-x}PbI_3$ (x=0—1) absorber layers

Fig.7 compares the Nyquist plots (in dark) of the PSC devices with various perovskite absorbers. After fitting with a simple equivalent circuit shown in the insert of Fig.7, the results are listed in Tab.2. It is observed that the Nyquist plots can be fitted well, where R_1 represents the series resistance, R_2 represents the charge transfer resistance from the HTM layer, while R_3 is associated with the charge recombination resistance from the interfaces of TiO_2/perovskite and perovskite/HTM. It is found that the PSC device containing a 12.5% FAI doped absorber displays the largest R_3 value, while there is no large difference in the R_1 and R_2 values among these PSC devices. It means that the interfacial charge recombination (or said, the leakage current) is suppressed a lot after doping appropriate FAI contents, which should be ascribed to the improved surface morphology of the perovskite absorbers.

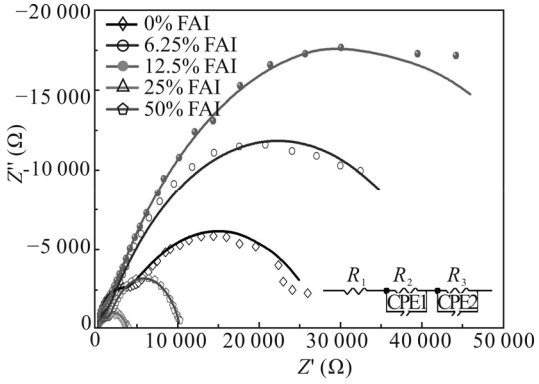

Fig.7 Nyquist plots of the PSC devices based on perovskite $(FA)_x(MA)_{1-x}PbI_3$ (x=0—0.5) absorber layers recorded in dark (The inset displays an equivalent circuit model for fitting, and the fitted plots are shown as solid lines.)

Tab.2 Calculated photovoltaic parameters from Fig.7

Sample	R_1 / Ω	R_2 / Ω	R_3 / Ω
0% FAI	4.6	1 819	26 558
6.25% FAI	22.5	767	43 325
12.5% FAI	22.8	689	61 530
25.0% FAI	11.3	781	3 342
50.0% FAI	6.9	1 437	8 951

Fig.8 displays the stability of an $MAPbI_3$ based PSC laid in vacuum for 10 days. The as-fabricated PSC device displays a *PCE* of 13.4%, which is enhanced firstly and then reduced. The enhancement might be associated with the improved interface contact or quality between the perovskite layer and HTM layer, as has been demonstrated in Ref[20]. Finally, a *PCE* of 11.27% still remains even after 10 days, suggesting that the PSCs fabricated in our lab own an excellent stability.

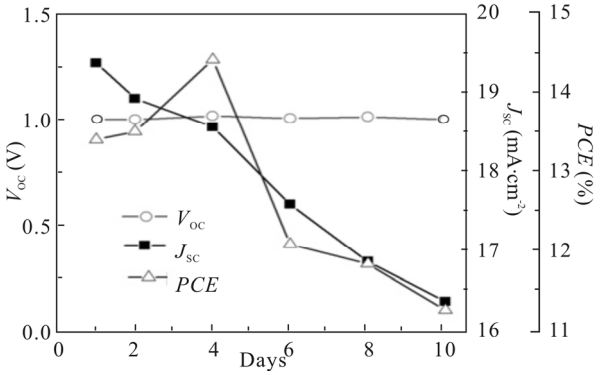

Fig.8 Stability measurements on the performance of a PSC device made with a single $MAPbI_3$ absorber layer which was laid in the vacuum environment for 10 days

The composition of a perovskite absorber layer was tuned continuously for enhancing the performance of a PSC device. It was found that the highest efficiency of 14.72% was achieved in the PSC devices with a nominal FAI content of 12.5 at.%. Compared with the single $MAPbI_3$ one, the performance enhancement was attributed to both the enhancement of visible-light absorption and carrier transport, which could be also demonstrated directly through the *IPCE* spectra and EIS results, respectively. Moreover, the device performance could be stable for at least 10 days in vacuum. We hope that our studies could help to understand the performance enhancement mechanism of a perovskite solar cell or other related photoelectric devices, such as light-emitting devices.

References

[1] I. Chung, B. Lee, J. He, R.P.H. Chang and M.G. Kanatzidis, Nature **485**, 486 (2012).

[2] M.M. Lee, J. Teuscher, T. Miyasaka, T.N. Murakami and H.J. Snaith, Science **338**, 643 (2012).

[3] H. Kim, C. Lee, J. Im, K. Lee, T. Moehl, A. Marchioro, S. Moon, R. Humphry-Baker, J. Yum, J.E. Moser, M. Graäzel and N. Park, Sci. Rep. **2**, 591 (2012).

[4] A. Kojima, K. Teshima, Y. Shirai and T. Miyasaka, J. Am. Chem. Soc. **131**, 6050 (2009).

[5] D. Bi, C. Yi, J. Luo, J. Décoppet, F. Zhang, S. M. Zakeeruddin, X. Li, A. Hagfeldt and M. Grätzel, Nat. Energy **1**, 16142 (2016).

[6] H. Chen, F. Ye, W. Tang, J. He, M. Yin, Y. Wang, F. Xie, E. Bi, X. Yang, M. Grätzel and L. Han, Nature **550**, 92 (2017).

[7] K.A. Bush, A.F. Palmstrom, Z.J. Yu, M. Boccard, R. Cheacharoen, J.P. Mailoa, D. P. McMeekin, R.L.Z. Hoye, C.D. Bailie, T. Leijtens, I.M. Peters, M.C. Minichetti, N. Rolston, R. Prasanna, S. Sofia, D. Harwood, W. Ma, F. Moghadam, H.J. Snaith, T. Buonassisi, Z.C. Holman, S.F. Bent and M.D. McGehee, Nat. Energy **2**, 17009 (2017).

[8] J. Luo, J. Im, M. T. Mayer, M. Schreier, M.K. Nazeeruddin, N. Park, S. David Tilley, H.J. Fan and M. Grätzel, Science **345**, 1593 (2014).

[9] Gurudaya, D. Sabba, M. Kumar, L.H. Wong, J. Barber, M. Grätzel and N. Mathews, Nano Lett. **15**, 3833 (2015).

[10] J.H. Kim, Y. Jo, J.H. Kim, J.W. Jang, H.J. Kang, Y.H. Lee, D.S. Kim, Y. Jun and J.S. Lee, Nature **9**, 11820 (2015).

[11] K. Jung, J. Seo, S. Lee, H. Shin and N. Park, J. Mater. Chem. A **5**, 24790 (2017).

[12] J.H. Heo, H.J. Han, M. Lee, M. Song, D.H. Kim and S.H. Im, Energy Environ. Sci. **8**, 2922 (2015).

[13] N.J. Jeon, J.H. Noh, W.S. Yang, Y.C. Kim, S. Ryu, J. Seo and S. II Seok, Nature **517**, 476 (2015).

[14] X. He, P. Guo, J. Wu, Y. Tu, Z. Lan, J. Lin and M. Huang, Sol. Energy **157**, 853 (2017).

[15] Y. Zhao, J. Wang, B. Zhao, C. Jia, J. Mou, L. Zhu, J. Song, X. Gu and Y. Qiang, Chinese Physics B **27**, 024208 (2018).

[16] S. Li, Y. Zhao, X. Gu, Y. Qiang and N. Tan, Journal of Materials Science: Materials in Electronics **28**, 13626 (2017).

[17] J. Song, S. P. Li, Y. L. Zhao, J. Yuan, Y. Zhu, Y. Fang, L. Zhu, X. Q. Gu and Y. H. Qiang, Journal of Alloys and Compounds **694**, 1232 (2017).

[18] Y. Yang, J. Song, Y. L. Zhao, L. Zhu, X. Q. Gu, Y. Q. Gu, M. Che and Y. H. Qiang, Journal of Alloys and Compounds **684**, 84 (2016).

[19] W. S. Yang, J. H. Noh, N. J. Jeon, Y. C. Kim, S. Ryu, J. Seo and S. Seok, Science **348**, 1234 (2015).

[20] W. Zhu, C. Bao, F. Li, T. Yu, H. Gao, Y. Yi, J. Yang, G. Fu, X. Zhou and Z. Zou, Nano Energy **19**, 17 (2016).